MCB
Journals.ASM.org

Activated Cdc42-Bound IQGAP1 Determines the Cellular Endocytic Site

Toshihide Kimura,[a] Mami Yamaoka,[a] Shigeki Taniguchi,[a] Mitsuhiro Okamoto,[a] Masahiro Takei,[a] Tomomi Ando,[a] Akihiro Iwamatsu,[b] Takashi Watanabe,[c] Kozo Kaibuchi,[c,d] Toshimasa Ishizaki,[a] Ichiro Niki[a]

Department of Pharmacology, Oita University Faculty of Medicine, Hasama, Yufu, Oita, Japan[a]; Protein Research Network, Inc., Midori-ku, Yokohama, Japan[b]; Department of Cell Pharmacology, Graduate School of Medicine, Nagoya University, Showa, Nagoya, Aichi, Japan[c]; JST, CREST, Kawaguchi, Japan[d]

Recruitment of specific molecules to a specific membrane site is essential for communication between specialized membranous organelles. In the present study, we identified IQGAP1 as a novel GDP-bound-Rab27a-interacting protein. We found that IQGAP1 interacts with GDP-bound Rab27a when it forms a complex with GTP-bound Cdc42. We also found that IQGAP1 regulates the endocytosis of insulin secretory membranes. Silencing of IQGAP1 inhibits both endocytosis and the glucose-induced redistribution of endocytic machinery, including Rab27a and its binding protein coronin 3. These processes can also be inhibited by disruption of the trimeric complex with dominant negative IQGAP1 and Cdc42. These results indicate that activation of Cdc42 in response to the insulin secretagogue glucose recruits endocytic machinery to IQGAP1 at the cell periphery and regulates endocytosis at this membrane site.

Targeting of specific molecules to specific cell membrane sites is essential for the generation of specialized membranous organelles and for communication between these organelles. The exocytic machinery is localized at both the secretory membrane and the plasma membrane. In pancreatic beta cells, glucose stimulation promotes the association of this machinery with the cell membrane, resulting in insulin release. Glucose stimulation also promotes the endocytosis of secretory membranes to maintain a constant cell volume and to allow the reuse of the exocytic machinery for another round of exocytosis (1, 2). Although these excess membranes and the used machinery are taken up by endocytic machinery, knowledge regarding the mechanism by which endocytic machinery is targeted to a specific membrane site is still limited.

Small GTPases are monomeric GTPases with molecular masses ranging from 20 to 30 kDa (3, 4). These molecules have GTP- and GDP-bound forms, and they interconvert between the two states. This conversion is regulated by GDP/GTP exchange and by GTPase reactions. It is conventionally considered that small GTPases are maintained in the GDP-bound form by guanine nucleotide dissociation inhibitors (GDIs) in the cytosol (5–7). Cell stimulation converts the GTPases from the GDP- to the GTP-bound form through their interaction with guanine nucleotide exchange factors (GEFs) (8). The GTP-bound form interacts with its specific GTP-dependent effectors and transduces a specific downstream signal. GTPase-activating proteins (GAPs) activate the intrinsic GTPase activity of small GTPases and induce the conversion of the GTP- to the GDP-bound form (9). There is a specific GDI, GEF, and GAP for each small GTPase, and these regulate the function and localization of the relevant GTPase.

Small GTPases are divided into the Ras, Rho, Rab, Arf, and Ran superfamilies, and each family participates in a wide variety of cellular functions (3). In pancreatic beta cells, the Rho family regulates cytoskeletal remodeling and the fusion event in exocytosis (10). Cdc42, a member of the Rho family, is localized with insulin secretory granules (11). The insulin secretagogue glucose converts GDP-bound Cdc42 to its GTP-bound form, resulting in insulin secretion through modulation of the cortical actin network (12). Cdc42 also regulates granule fusion via the soluble *N*-ethylmaleimide-sensitive factor attachment protein receptor (SNARE) protein (13). Furthermore, GTP-bound Cdc42 causes a shift of Rac-1, another member of the Rho family, from the GDP- to the GTP-bound form (14). IQGAP1 is one of the GTP-dependent effectors of Cdc42 and Rac1 (15, 16). IQGAP1 regulates cell-cell contacts and cell migration (17–21). In pancreatic beta cells, IQGAP1 forms a complex with exocysts, and GTP-bound Cdc42 abolishes this association (22). Thus, IQGAP1 is involved in the regulation of vesicle tethering in insulin secretion (22, 23).

The Rab family, which consists of more than 60 members, regulates membrane trafficking via its specific effectors (24–26). Rab27a, a member of the Rab family, is highly expressed in pancreatic beta cells and is involved in the preexocytosis of insulin granules via its specific effectors. Exophilin8/MyRIP/Slac2c, Noc2, and granuphilin/Slp4 have been identified as Rab27a effectors in pancreatic beta cells (27). Exophilin8/MyRIP/Slac2c functions as a linker protein between GTP-bound Rab27a and motor proteins such as myosin Va, which may transport insulin granules along actin filaments (28, 29). Noc2 is considered to regulate insulin secretion by modulating actin dynamics via zyxin (30, 31). Granuphilin/Slp4 plays an inhibitory role in the secretory machinery via the tethering of insulin granules to the cytoplasmic surface of the cell membrane (32–34). All known effectors are considered to be GTP-dependent effectors (24).

We recently identified coronin 3 as a GDP-bound-Rab27a-interacting protein (1, 2). We showed that the insulin secreta-

Received 11 July 2013 Returned for modification 29 July 2013
Accepted 1 October 2013
Published ahead of print 7 October 2013
Address correspondence to Toshihide Kimura, t-kimura@oita-u.ac.jp.
Supplemental material for this article may be found at http://dx.doi.org/10.1128/MCB.00895-13.

doi:10.1128/MCB.00895-13

gogue glucose induces the conversion of GTP-bound Rab27a to GDP-bound Rab27a, which is essential for the redistribution of coronin 3 to the vicinity of the plasma membrane (35, 36). We also showed that GDP-bound Rab27a promotes the F-actin-bundling activity of coronin 3, resulting in regulation of the endocytosis of insulin secretory membranes (37).

In this study, we identified IQGAP1 as a novel GDP-dependent effector of Rab27a. We found that Cdc42-induced activation of IQGAP1 regulates the glucose-induced redistribution of Rab27a and coronin 3. We also found that the Cdc42-induced formation of a complex between IQGAP1, GDP-bound Rab27a, and coronin 3 is essential for endocytosis of the insulin secretory membrane. Here we suggest that activated Cdc42-bound IQGAP1 determines the cellular endocytic site via the recruitment of endocytic machinery.

MATERIALS AND METHODS

Materials. pAcGFP and pmCherry were purchased from Clontech. pcDNA3.1/Hygro(−) was purchased from Invitrogen, pGEX-4T-1 was purchased from GE Healthcare Ltd., and pMAL-p4x was purchased from New England Biolabs. pQE30 was purchased from Qiagen. A polyclonal anti-coronin 3 antibody was produced as described previously (35). The following antibodies were used: polyclonal anti-Rab27a (H-60), anti-Flag (M2), antiactin (AC-15), and anti-glutathione *S*-transferase (anti-GST) (GST-2) antibodies (Sigma-Aldrich); monoclonal anti-Rab27a (1G7) and monoclonal anti-coronin 3 (1F7) antibodies (Abnova); a polyclonal antibody against green fluorescent protein (GFP) (MBL); an anti-T7 antibody (Novagen); antibodies against IQGAP1 (H-109) and maltose-binding protein (MBP) (Santa Cruz); a monoclonal anti-GFP antibody (Roche); an anti-His antibody (Qiagen); an anti-Cdc42 antibody (Thermo Scientific); and an anti-insulin antibody (Seikagaku Corporation). COS-7 cells were obtained from the Cell Resource Center for Biomedical Research, Tohoku University. The insulin-secreting beta-cell line MIN6 was kindly provided by J. I. Miyazaki (Osaka University). Other materials and chemicals were obtained from commercial sources. This study was approved by the Ethical Committee for Animal Experiments at Oita University.

Plasmid constructs. cDNAs encoding Rab27a, coronin 3, Rab5a (35), IQGAP1, RhoA, and Cdc42 (38) were obtained as described previously. cDNA encoding rat phogrin was kindly provided by E. Kawasaki (Nagasaki University). pFLAG-CMV-2b-Rab3a was kindly provided by S. Seino (Kobe University) (31). pEGFP-phogrin was kindly provided by T. Senda (Fujita Health University School of Medicine). pcDNA-Flag and pcDNA-T7 were generated as described previously (35). The cDNAs encoding the IQGAP1 calponin homology domain (CHD), N-terminal repeats (NTR), isoleucine and glutamine repeats (IQR), GTPase-related domain (GRD), and carboxy terminus (CT) were amplified by PCR. All DNA point mutations were introduced using a QuikChange kit (Stratagene). An RNA interference-resistant mutant of IQGAP1 ($RNAi^R$-IQGAP1) was created by introducing three silent mutations (underlined in the sequence) into human IQGAP1 at nucleotides 3268 to 3292 (5′-G ACCCAGTGGACATTTATAAATCTT-3′).

Protein purification. GST fusion proteins, MBP fusion proteins, and His-tagged and Flag-tagged proteins were purified according to the manufacturer's protocol. GST-IQGAP1 was purified from *Spodoptera frugiperda* cells, which express this protein, as described previously (38).

Affinity column chromatography. Affinity column chromatography was carried out as described previously (35). In brief, MIN6 cell membrane fractions were loaded onto glutathione-Sepharose 4B beads (GE Healthcare) coated with GST or GDP·GST-Rab27a. The columns were washed with NS-buffer (20 mM HEPES at pH 7.5, 5 mM $MgCl_2$, 1 mM dithiothreitol [DTT], 100 mM NaCl, 1 mM GDP). The proteins bound to the columns were eluted with NS-buffer containing 1.5 M NaCl and were analyzed by peptide mass fingerprinting.

Coimmunoprecipitation assay. Immunoprecipitation was performed as described previously (35). In brief, MIN6 cells were extracted by the addition of L1-buffer (20 mM Tris at pH 7.5, 150 mM NaCl, 1 mM EDTA, 1 μM phenylmethylsulfonyl fluoride [PMSF], 10 μg/ml leupeptin, 10 μg/ml aprotinin, and 1% NP-40) and were incubated with a polyclonal anti-Rab27a or anti-IQGAP1 antibody. The immunocomplex was then precipitated with protein A-Sepharose 4B (GE Healthcare). The bound proteins were eluted using L1-buffer containing 0.5 M NaCl and were subjected to immunoblotting with a polyclonal anti-Rab27a, anti-IQGAP1, anti-Cdc42, or anti-coronin 3 antibody. For this blot, 0.7% of the total lysate was loaded as input.

Cell culture and transfection. COS-7 and MIN6 cells were cultured in Dulbecco's modified Eagle's medium (Sigma-Aldrich) supplemented with 10% and 15% fetal bovine serum, respectively. Lipofectamine 2000 (Invitrogen) reagents were used for transfection according to the manufacturer's instructions.

Binding assay. Immunoprecipitation was performed as described previously (35). In brief, COS-7 cells expressing GFP-IQGAP1 mutants, Flag-Rab mutants, and T7-Rho mutants were solubilized with L2-buffer (20 mM Tris at pH 7.5, 100 mM NaCl, 1 mM EDTA, 1 μM PMSF, 10 μg/ml leupeptin, 10 μg/ml aprotinin, and 0.1% NP-40). GFP-IQGAP1 mutant proteins were immunoprecipitated with a polyclonal anti-GFP antibody. The immunocomplex was subjected to immunoblotting with a monoclonal anti-GFP, anti-Flag, or anti-T7 antibody. For this blot, 0.7% of the total was loaded as input. For the direct binding assay using purified recombinant proteins, glutathione-Sepharose 4B beads coated with GST or GST-Rab27a were incubated with MBP-IQGAP1-GRD in L3-buffer (50 mM HEPES at pH 7.5, 150 mM NaCl, 1 μM PMSF, 10 μg/ml leupeptin, 10 μg/ml aprotinin, and 0.1% NP-40) at 4°C for 1 h. The beads were then washed with L3-buffer and were resuspended with SDS-PAGE sampling buffer. The bound proteins were subjected to immunoblot analysis with an anti-MBP antibody. The *in vitro* binding assays using MBP-Rho mutants, His-Rab27a-T23N, purified Flag-coronin 3, and GST-IQGAP1 immobilized on beads were performed in the same way.

Endocytosis assay. The Neon transfection system (Life Technologies) was used for transfection according to the manufacturer's instructions. The cell surface proteins were biotinylated using EZ-Link sulfo-NHS-SS-biotin (Pierce) for 30 min at 4°C, after which the unreacted biotin was quenched (1% bovine serum albumin [BSA] in phosphate-buffered saline [PBS]). The samples were warmed to 37°C to allow endocytosis. The remaining cell surface biotin was stripped using L4 buffer (50 mM Tris, 100 mM sodium 2-mercaptoethanesulfonate, 100 mM NaCl, 1 mM EDTA, 0.2% BSA), after which the cells were lysed and the endocytosed biotin-tagged proteins were pulled down using streptavidin-agarose. The endocytosed proteins were determined by SDS-PAGE and subsequent densitometry.

Immunohistochemistry. Pancreata from male ICR mice (SLC), aged 8 to 12 weeks, were fixed with phosphate-buffered 3% paraformaldehyde and were cryosectioned at a thickness of 5 μm. The tissue sections were subjected to immunostaining. Cryosections of the fixed pancreata were incubated with a mixture of a guinea pig anti-insulin antibody and a rabbit anti-IQGAP1 antibody, followed by incubation with a mixture of Alexa Fluor 568-conjugated anti-guinea pig IgG and Alexa Fluor 488-conjugated anti-rabbit IgG (Molecular Probes).

siRNA preparation. Coronin-3-specific small interfering RNA (siRNA) was synthesized as described previously (35). siRNAs specific to Rab27a (MSS202211) and IQGAP1 (MSS219911) were purchased from Invitrogen. NegaConNaito1 (RNAi Co., Ltd.) was used as a negative control.

Immunofluorescence analyses. Immunofluorescence analyses were performed as described previously (36). In brief, MIN6 cells expressing GFP- or Flag-tagged proteins were preincubated with HEPES-buffered Krebs buffer (20 mM HEPES at pH 7.4, 119 mM NaCl, 4.8 mM KCl, 2.5 mM $CaCl_2$, 1.2 mM $MgSO_4$, 1.2 mM KH_2PO_4, 5 mM $NaHCO_3$, and 1 mg/ml BSA) with 3 mM glucose, followed by incubation with the same buffer with 20 mM glucose. The cells were then rinsed in phosphate-

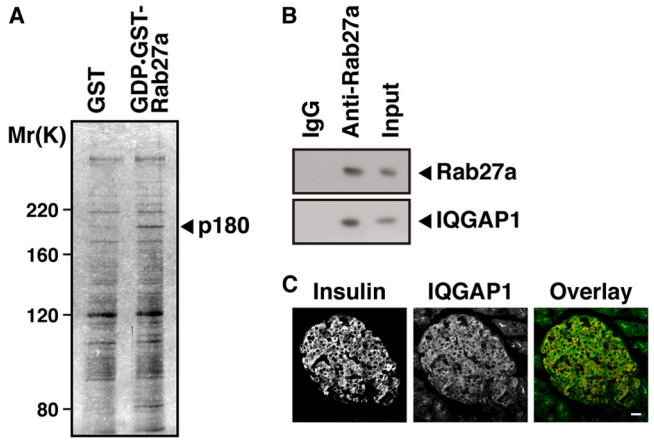

FIG 1 Identification of IQGAP1 as a protein interacting with GDP-bound Rab27a in pancreatic beta cells. (A) MIN6 cell extracts were applied to an affinity column on which GST-tagged GDP-bound Rab27a or GST alone (as a control) was immobilized, and eluates were analyzed by silver staining. (B) MIN6 extracts were immunoprecipitated with an anti-Rab27a antibody or with control IgG. The immunocomplexes were analyzed by immunoblotting with an anti-Rab27a or anti-IQGAP1 antibody. The percentage of input protein coimmunoprecipitated was 0.2%. (C) Sections of mouse pancreata were double stained with anti-insulin (red) and anti-IQGAP1 (green) antibodies. Bar, 20 μm.

buffered saline, fixed with 3% paraformaldehyde, permeabilized with 0.1% Triton X-100, and stained with anti-Flag and anti-IQGAP1 antibodies, followed by Alexa Fluor 488- and Alexa Fluor 568-conjugated secondary antibodies. We traced the intracellular fluorescence signals and performed statistical analyses as described previously (36). Cells with obvious peaks in the vicinity of the plasma membrane were counted. We defined the vicinity of the plasma membrane as the outermost 10% of the cell area (39). The FM4-64 uptake experiments were performed as described previously (35). In brief, MIN6 cells were incubated in culture media containing 10 μM FM4-64. The cells were then thoroughly washed with dye-free media and were used for live imaging. For transferrin uptake experiments, MIN6 cells were incubated in HEPES-buffered Krebs buffer with 20 mM glucose and 5 μg/ml Alexa Fluor 568-labeled transferrin for 30 min. The cells were then thoroughly washed with phosphate-buffered saline and were fixed with 3% paraformaldehyde. For analysis of phogrin-Cherry internalization, FM4-64 uptake, and transferrin uptake, the percentage of cells with a cytoplasmic pattern of staining of these molecules was evaluated (35).

Confocal fluorescence microscopy. Images were acquired using a 100× oil objective (Plan-Apochromat 100× [numerical aperture, 1.46] oil immersion objective for differential interference contrast [DIC]; Carl Zeiss). All sections were analyzed using a confocal laser microscopy system and software (LSM710; Carl Zeiss) that was built around an inverted microscope (Axio Observer Z1; Carl Zeiss).

Statistical analysis. All data are expressed as means ± standard deviations (SD). Data were evaluated for statistical significance using the unpaired Student *t* test.

RESULTS

IQGAP1 is a novel GDP-bound-Rab27a-interacting protein. We first searched for GDP-bound-Rab27a-interacting proteins in pancreatic beta cells by using affinity column chromatography and peptide mass fingerprinting. Extracts from the insulin-secreting beta-cell line MIN6 were applied to a column to which GST-tagged GDP-bound Rab27a (GDP·GST-Rab27a) was immobilized. A protein with a relative molecular weight (M_r) of 180,000 (p180) bound GDP–GST-Rab27a but not GST alone (Fig. 1A). We identified p180 as IQGAP1 by peptide mass fingerprinting (see Fig. S1 in the supplemental material). A coimmunoprecipitation assay using MIN6 extracts was performed to determine if Rab27a forms a complex with IQGAP1 in MIN6 cells. Indeed, IQGAP1 was found to coimmunoprecipitate with the anti-Rab27a antibody (Fig. 1B). The cellular distribution of IQGAP1 in the mouse pancreas was examined by immunohistochemical analysis (Fig. 1C). IQGAP1 was preferentially expressed in the islet cells. The immunofluorescence of IQGAP1, like that of Rab27a (35), was observed in insulin-positive beta cells as well as in other types of islet cells.

We next performed a cotransfection assay in COS-7 cells to determine the GTP/GDP specificity of the interaction between Rab27a and IQGAP1. Briefly, Flag-Rab27a-Q78L, a GTPase-deficient mutant that mimics the GTP-bound state, or Flag-Rab27a-T23N, which mimics the GDP-bound state, was cotransfected with GFP-IQGAP1 into COS-7 cells, and the association of each mutant with IQGAP1 was evaluated following immunoprecipitation with the anti-GFP antibody (Fig. 2A). Rab27a-T23N coimmunoprecipitated with IQGAP1, but Rab27a-Q78L did not. Rab27a-Q78L did coimmunoprecipitate with the synaptotagmin-like protein homology domain (SHD), which is the GTP-bound-Rab27a-binding domain of the GTP-dependent effectors of Rab27a (40), indicating that IQGAP1 specifically binds Rab27a in a GDP-dependent manner. Only a small amount of GDP-bound Rab3a (Rab3a-T36N), which has the highest homology to Rab27a among the Rab family (40% similarity to the amino acid sequence of Rab27a), but not GDP-bound Rab5a (Rab5a-S34N), coimmunoprecipitated with IQGAP1, indicating that IQGAP1 preferentially interacts with Rab27a *in vivo*.

We also identified the sites required for the interaction with IQGAP1 by using cotransfection assays in COS-7 cells (Fig. 2B). Rab27a-T23N bound IQGAP1-GRD (amino acids 925 to 1325) but not GFP or IQGAP1-CHD (amino acids 1 to 198), NTR (amino acids 175 to 726), IQR (amino acids 700 to 958), or CT (amino acids 1305 to 1658).

We then examined whether IQGAP1 directly binds GDP-bound Rab27a by using an *in vitro* binding assay with purified recombinant proteins. IQGAP1 bound GDP-bound Rab27a but not GST alone or Rab27a treated with the nonhydrolyzable GTP analogue GTPγS (Fig. 2C). The binding of IQGAP1 to GDP-bound Rab27a was dose dependent and saturable (Fig. 2D). The dissociation constant (K_d) determined by Scatchard analysis was 0.2 μM, and the stoichiometry was 0.01. This K_d value is almost the same as that for the binding affinity of coronin 3 for GDP-bound Rab27a (35). The K_d value of IQGAP1 binding to GDP-bound Rab3a (0.8 μM) was 4 times lower than that of IQGAP1 binding to GDP-bound Rab27a (Fig. 2E). This result is consistent with the results from our coimmunoprecipitation experiments (Fig. 2A).

IQGAP1 is required for the glucose-induced redistribution of Rab27a and coronin 3. We have demonstrated previously that glucose, the most important insulin secretagogue, induces the intracellular translocation of coronin 3 and that this redistribution is due to the interaction of coronin 3 with GDP-bound Rab27a (36). We therefore examined the intracellular distribution of IQGAP1 in MIN6 cells. In this set of experiments, IQGAP1-silenced MIN6 cells were cotransfected with Flag-Rab27a. IQGAP1 with RNA interference (RNAi) diminished the expression of endogenous IQGAP1 by 70% without affecting the expression of the

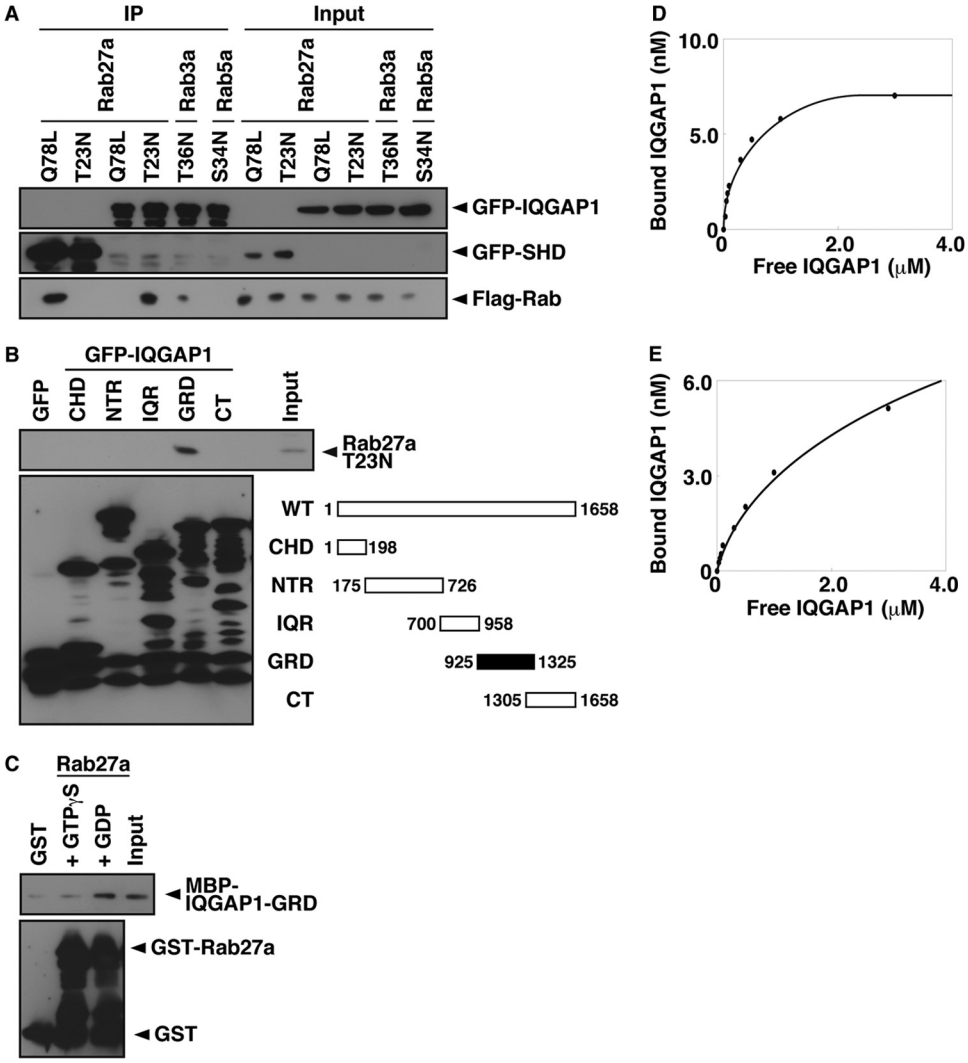

FIG 2 IQGAP1-GRD binds GDP-bound Rab27a. (A) COS-7 extracts expressing Flag-Rab mutants and GFP-SHD (lanes 1 and 2) or GFP-IQGAP1 (lanes 3 to 6) were immunoprecipitated (IP) with an anti-GFP antibody. The immunocomplexes were analyzed by immunoblotting using anti-GFP and anti-Flag antibodies. The percentage of input protein coimmunoprecipitated was 0.2%, except for the T36N mutant (0.02%). (B) COS-7 extracts expressing Flag-Rab27a-T23N and GFP-IQGAP1 deletion mutants were immunoprecipitated with an anti-GFP antibody. The immunocomplexes were analyzed by immunoblotting using anti-Flag and anti-GFP antibodies. Two percent of input protein was coimmunoprecipitated. Abbreviations for IGAP1 domains are as follows: CHD, calponin homology domain; NTR, N-terminal repeats; IQR, IQ repeats; GRD, GTPase-related domain; CT, carboxy terminus. (C) An *in vitro* binding assay was performed using purified MBP-IQGAP1-GRD and bead-bound GST-Rab27a, and bead-bound proteins were immunoblotted with anti-MBP and anti-GST antibodies. (D and E) *In vitro* binding assays using various concentrations of MBP-IQGAP1-GRD and GST-Rab27a-T23N (D) or GST-Rab3a-T36N (E).

endogenous proteins coronin 3, actin, and Rab27a (Fig. 3A). In control cells, glucose stimulation induced the redistribution of Flag-Rab27a to the vicinity of the plasma membrane, where IQGAP1 accumulated (Fig. 3B and C). This Rab27a redistribution did not occur in IQGAP1-silenced cells. In contrast, IQGAP1 was distributed in the vicinity of the plasma membrane in both stimulated and unstimulated cells. We also examined the glucose-induced redistribution of endogenous insulin granules and Rab27a (see Fig. S2A in the supplemental material). Insulin granules were also redistributed in glucose-stimulated MIN6 cells. These results suggest that IQGAP1 may regulate the glucose-induced translocation of Rab27a.

To verify this effect of IQGAP1, an RNAi-resistant ($RNAi^R$) mutant of IQGAP1 was constructed by introducing a silencing mutation into IQGAP1 at the target sequence of the siRNA. Although GFP-IQGAP1 expression was abolished by IQGAP1 siRNA (siIQGAP1), the expression of GFP-$RNAi^R$-IQGAP1 persisted (Fig. 3D). The inhibition by siIQGAP1 of the glucose-induced redistribution of Rab27a was reversed when cells were cotransfected with $RNAi^R$-IQGAP1 (Fig. 3E and F).

We showed previously that the glucose-induced redistribution of coronin 3 does not occur in Rab27a-silenced cells (36). We therefore examined the effect of IQGAP1 on the distribution of coronin 3 in MIN6 cells. The glucose-induced redistribution of coronin 3 was also inhibited in IQGAP1-silenced cells (see Fig. S2B and C in the supplemental material), and this inhibition was reversed when the cells were cotransfected with $RNAi^R$-IQGAP1 (see Fig. S2D and E in the supplemental material). However, the localization of IQGAP1 was not affected in cells in which either Rab27a or coronin 3 was silenced (see Fig. S2F to H). Moreover,

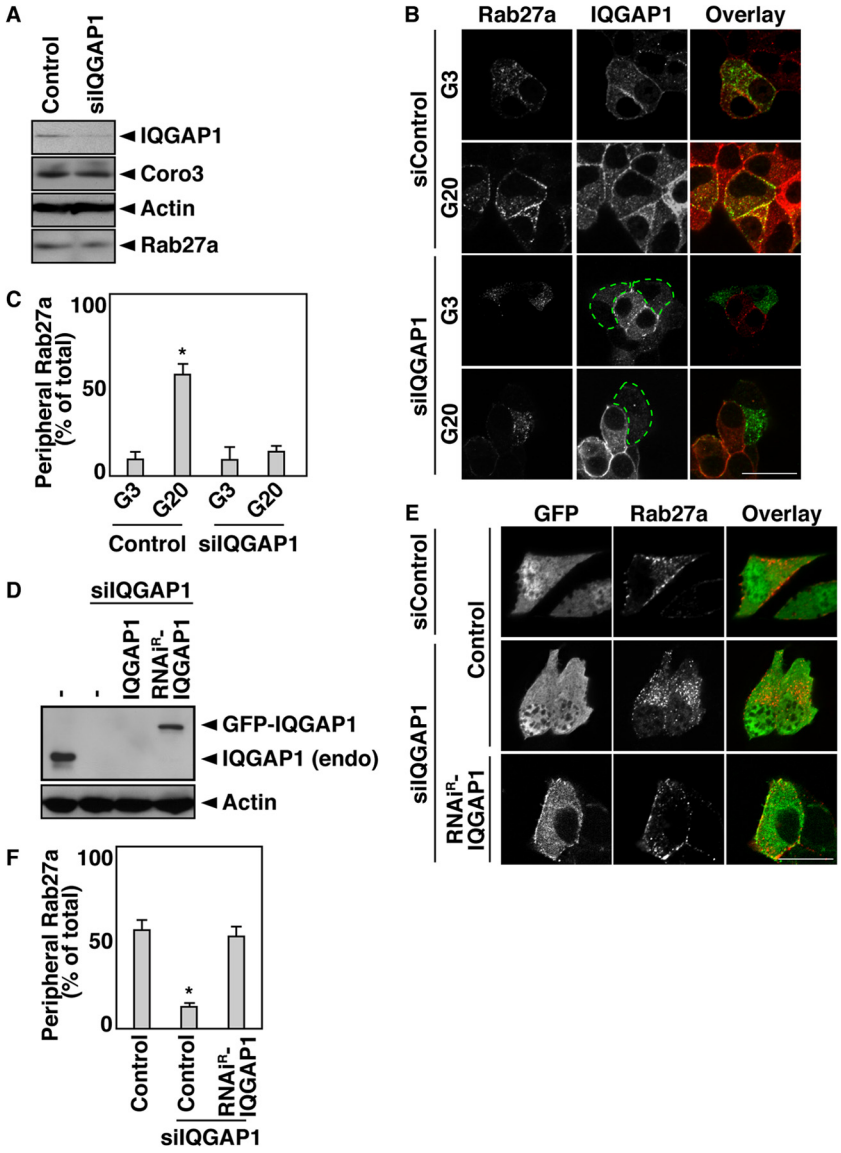

FIG 3 IQGAP1 is required for the glucose-induced redistribution of Rab27a. (A) IQGAP1-silenced MIN6 cells were analyzed by immunoblotting with anti-IQGAP1, anti-coronin 3 (Coro3), antiactin, and anti-Rab27a antibodies. (B) IQGAP1-silenced MIN6 cells expressing Flag-Rab27a were incubated with 3 or 20 mM glucose (G3 or G20, respectively) for 5 min. The cells were immunostained with anti-Flag (green) and anti-IQGAP1 (red) antibodies. siControl, control siRNA. (C) The percentage of cells analyzed as in panel B with a peripheral distribution of Flag-Rab27a was determined. The results of statistical analysis of the percentage of transfected cells that had Rab27a near the plasma membrane are shown. More than 40 randomly selected cells (more than 8 cells/experiment) were examined. Data are expressed as means ± SD from 4 independent experiments. The asterisk indicates a significant difference (P, <0.01) from siControl cells stimulated with 3 mM glucose by the unpaired Student t test. (D) IQGAP1-silenced MIN6 cells expressing GFP-IQGAP1 or GFP-RNAi^R-IQGAP1 were analyzed by immunoblotting using anti-IQGAP1 and antiactin antibodies. −, GFP. (E) IQGAP1-silenced MIN6 cells expressing Flag-Rab27a and GFP or GFP-RNAi^R-IQGAP1 were incubated with 20 mM glucose for 5 min. The cells were immunostained with an anti-Flag antibody (red). Control, GFP. Bars, 10 μm. (F) The percentage of cells analyzed as in panel E with a peripheral distribution pattern of Flag-Rab27a was determined. Statistical analysis was performed as described for panel C. Control, GFP. The asterisk indicates a significant difference (P, <0.01) from siControl-expressing cells by the unpaired Student t test.

the introduction of siRNAs against IQGAP1, Rab27a, or coronin 3 did not affect the cortical actin network (see Fig. S3A in the supplemental material). These results indicate that IQGAP1 is required for the glucose-induced redistribution of Rab27a and its binding protein coronin 3.

Cdc42 regulates the interaction between IQGAP1 and GDP-bound Rab27a. IQGAP1 is a GTP-dependent effector of Rac1 and Cdc42 (15, 16), which are members of the Rho family of GTPases. An *in vitro* binding assay showed that Rab27a-T23N bound IQGAP1 when the latter formed a complex with Cdc42-G12V, a GTPase-deficient mutant that mimics the GTP-bound state (Fig. 4A). This interaction was not detected in the presence of another Rho family GTPase, RhoA, or in the presence of Cdc42-T17N, a mutant that mimics the GDP-bound state. We found that this interaction was also detected in the presence of Rac1-G12V. Stimulation with glucose for 2 min converts Cdc42 from its GDP-bound form to a GTP-bound form in MIN6 cells (12). At the same time, glucose stimulation converts GTP-bound Rab27a to its

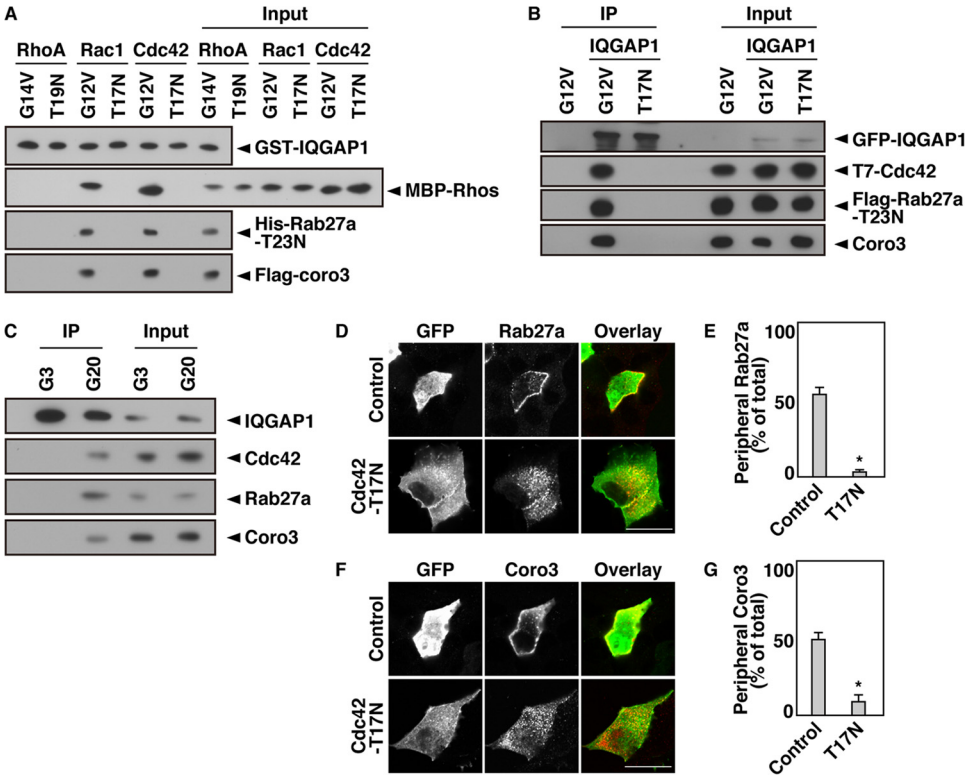

FIG 4 Cdc42 regulates the interaction between IQGAP1 and GDP-bound Rab27a. (A) An *in vitro* binding assay was performed using purified bead-bound GST-IQGAP1, His-Rab27a-T23N, Flag-coronin 3, and an MBP-tagged RhoA, Rac1, or Cdc42 mutant. Following incubation, bead-bound proteins were analyzed by immunoblotting using anti-GST, anti-MBP, anti-His, and anti-Flag antibodies. (B) COS-7 extracts expressing GFP-IQGAP1, Flag-Rab27a-T23N, and one of the T7-Cdc42 mutants (the G12V or T17N mutant) were immunoprecipitated with an anti-GFP antibody. The immunocomplexes were analyzed by immunoblotting using anti-GFP, anti-T7, anti-Flag, and anti-coronin 3 antibodies. The percentage of input protein coimmunoprecipitated was 0.2%. (C) MIN6 cells were incubated with 3 or 20 mM glucose for 5 min. The cell extracts were immunoprecipitated with an anti-IQGAP1 antibody. The immunocomplexes were analyzed by immunoblotting with anti-IQGAP1, anti-Cdc42, anti-Rab27a, and anti-coronin 3 antibodies. The percentage of input protein coimmunoprecipitated was 0.1%. (D) MIN6 cells expressing Flag-Rab27a together with GFP or GFP-Cdc42-T17N were incubated with 20 mM glucose for 5 min. The cells were immunostained with an anti-Flag (red) antibody. (E) The percentage of cells with a peripheral distribution pattern of Flag-Rab27a was analyzed. (F) MIN6 cells expressing Flag-coronin 3 together with GFP or GFP-Cdc42-T17N were incubated with 20 mM glucose for 5 min. The cells were immunostained with an anti-Flag (red) antibody. Bars, 10 μm. (G) The percentage of cells with a peripheral distribution pattern of Flag-coronin 3 was analyzed. Peripheral distribution and statistical analyses were performed as described in the legend to Fig. 3C.

GDP-bound form (35). On the other hand, glucose-induced Rac1 activation requires 20 min (14). We therefore examined the effect of GTP-bound Cdc42 on the interaction between IQGAP1 and GDP-bound Rab27a. The interaction between IQGAP1 and Rab27a-T23N was also promoted in Cdc42-G12V-expressing cells but not in Cdc42-T17N-expressing cells (Fig. 4B). This complex formation was also detected in glucose-stimulated MIN6 cells (Fig. 4C). These results indicate that GDP-bound Rab27a interacts with IQGAP1 only when IQGAP1 forms a complex with GTP-bound Cdc42. Glucose-induced redistribution of Rab27a and coronin 3 did not occur in Cdc42-T17N-expressing cells (Fig. 4D to G). Moreover, the expression of Cdc42-T17N did not affect the cortical actin network under these conditions (see Fig. S3A in the supplemental material). Neither L-glucose nor 2-deoxyglucose stimulation induced the redistribution of Rab27a to the vicinity of the plasma membrane (see Fig. S3B). This result is consistent with a previous result showing that Cdc42 activation is selective for glucose (14). These results indicate that GTP-bound Cdc42 forms a complex with IQGAP1 and recruits GDP-Rab27a and coronin 3 to the vicinity of the plasma membrane.

Coronin 3 was also detected in the complex that contained GTP-bound Cdc42, IQGAP1, and GDP-bound Rab27a (Fig. 4A to C). Rab27a-T23N efficiently bound coronin 3 in IQGAP1-GRD-expressing cells (see Fig. S3C in the supplemental material). However, coronin 3 did not directly bind IQGAP1-GRD. These results suggest that GDP-bound Rab27a binds both IQGAP1 and coronin 3 simultaneously and that they form a trimeric complex.

The complex consisting of IQGAP1 and GDP-bound Rab27a regulates endocytosis. We reported previously that coronin 3 forms a complex with GDP-bound Rab27a and that the complex regulates the endocytosis of secretory membranes in MIN6 cells (35–37). We therefore examined the effect of IQGAP1 silencing on endocytosis. IQGAP1-silenced MIN6 cells that expressed GFP as a transfection marker were labeled with FM4-64 to visualize endocytosis (see Fig. S4A and B in the supplemental material). FM4-64 was taken up by endocytosis and showed a punctate pattern in control cells, in agreement with our previous report (35). The uptake of FM4-64 was inhibited in IQGAP1-silenced cells. To further examine the role of IQGAP1 in endocytosis, IQGAP1-silenced MIN6 cells were incubated with Alexa Fluor 568-labeled transferrin for the visualization of clathrin-dependent endocytosis (see Fig. S4C and D). The uptake of transferrin was inhibited in

IQGAP1-silenced cells. Moreover, this inhibition of uptake was reversed by coexpression of RNAi^R-IQGAP1. Phogrin, a transmembrane protein, is a marker of secretory membranes (35). Following insulin exocytosis, phogrin is internalized by clathrin-dependent endocytosis (41, 42). Phogrin-Cherry was localized in the cytoplasm in control cells (see Fig. S4E and F), in agreement with our previous report (35). However, in IQGAP1-silenced cells, phogrin-Cherry was present near the plasma membrane. This change in phogrin distribution was reversed when the cells were cotransfected with RNAi^R-IQGAP1 (see Fig. S4E and F). Moreover, we directly evaluated the effect of IQGAP1 silencing on the endocytosis of secretory membranes by biotinylating phogrin at the plasma membrane and determining the fraction of phogrin endocytosed (see Fig. S4G and H). The silencing of IQGAP1 inhibited the endocytosis of phogrin (see Fig. S4G and H). In contrast, the levels of Kir6.2, the subunit of the ATP-sensitive potassium channel, remained unchanged (see Fig. S4G). These results indicate that IQGAP1 regulates the endocytosis of secretory membranes similarly to that of coronin 3 (35). The effect of siIQGAP1 on endocytosis may be secondarily affected, because IQGAP1 also regulates insulin secretion via exocysts (22). We therefore performed experiments using IQGAP1-GRD and Cdc42-T17N. These two mutants do not affect on the formation of the IQGAP1/exocyst complex (12, 22).

We examined whether the complex consisting of IQGAP1 and GDP-bound Rab27a regulates the endocytosis of secretory membranes. The uptake of transferrin was inhibited when the interaction between endogenous IQGAP1 and GDP-bound Rab27a was disrupted by the expression of Cdc42-T17N (see Fig. S5A and B in the supplemental material). Phogrin-Cherry was located mainly near the plasma membrane in cells expressing Cdc42-T17N (Fig. 5A and B). Moreover, the expression of Cdc42-T17N inhibited the endocytosis of phogrin (see Fig. S5C and D). In contrast, the levels of Kir6.2 remained unchanged (see Fig. S5C).

GFP-IQGAP1-GRD, which is the GDP-Rab27a binding site of IQGAP1 (Fig. 2B), bound Rab27a-T23N more efficiently than wild-type (WT) GFP-IQGAP1 (Fig. 5C). Moreover, Cdc42-G12V was not required for this interaction (Fig. 5C). The expression of IQGAP1-GRD disrupted the interaction between IQGAP1 and Rab27a-T23N (Fig. 5D), indicating that IQGAP1-GRD serves as a dominant negative deletion mutant. Indeed, glucose-induced redistribution of Rab27a and coronin 3 was inhibited by coexpression of IQGAP1-GRD (see Fig. S5E to H in the supplemental material). The uptake of transferrin was inhibited in IQGAP1-GRD-expressing cells (see Fig. S5A and B). Phogrin-Cherry was located mainly near the plasma membrane in these cells (Fig. 5E and F). Moreover, the expression of IQGAP1-GRD inhibited the endocytosis of phogrin (see Fig. S5C and D). In contrast, the levels of Kir6.2 remained unchanged (see Fig. S5C). These results indicate that the interaction between IQGAP1 and GDP-bound Rab27a is required for the endocytosis of secretory membranes.

DISCUSSION

IQGAP1, GDP-bound Rab27a, and coronin 3 regulate endocytosis. In the present study, IQGAP1 bound GDP-bound Rab27a when IQGAP1 formed a complex with GTP-bound Cdc42 (Fig. 4A to C). This interaction resulted in the recruitment of GDP-bound Rab27a from the cytosol to the plasma membrane, where IQGAP1 accumulated (Fig. 4D and E). IQGAP1 also recruited coronin 3, another GDP-bound-Rab27a-interacting protein, to the same area (Fig. 4F and G; see also Fig. S2 in the supplemental material). This finding was consistent with our previous results showing that glucose-induced translocation of coronin 3 is due to its interaction with GDP-bound Rab27a (36). Interestingly, IQGAP1 bound coronin 3 via GDP-bound Rab27a, thereby forming a trimeric complex (Fig. 4A to C; see also Fig. S3C in the supplemental material). Moreover, the interaction between coronin 3 and GDP-bound Rab27a was promoted when IQGAP1 was present (see Fig. S3C). These data suggested that coronin 3 bound GDP-bound Rab27a only when GDP-bound Rab27a formed a complex with IQGAP1 in the vicinity of the plasma membrane (Fig. 5G). These results indicate that GDP-bound Rab27a interacts with IQGAP1 in a fashion different from the interaction of coronin 3. Indeed, GRD has no homology with the beta-propeller structure, which is the binding site of coronin 3 to GDP-bound Rab27a (35, 40).

IQGAP1 is a scaffolding protein. IQGAP1 recruits signal molecules to specific areas within various cells where the accumulated molecules regulate their specific cellular functions, including cell motility (43), exocytosis (22), and phagocytosis (44). In pancreatic beta cells, IQGAP1 recruits vesicle-tethering exocysts (22). It has been reported that stable attachment of insulin granules to the plasma membrane is not a prerequisite but is temporally inhibitory for glucose-induced membrane fusion (45). Therefore, the complex may inhibit subsequent fusion events. The insulin secretagogue glucose causes a shift in Cdc42 from its GDP-bound to its GTP-bound form (12). This GTP-bound form interacts with IQGAP1 and disrupts the formation of the complex (22).

In this report, we demonstrated for the first time that IQGAP1 plays a crucial role in the control of endocytosis in pancreatic beta cells. We showed previously that glucose induces the intracellular translocation of coronin 3 from the cytosol to the plasma membrane (36). We also showed that peripheral coronin 3 contributes to the endocytosis of the secretory membrane by modulating F-actin (37). These data suggest that IQGAP1 determines the endocytic site via the recruitment of endocytic machinery, including GDP-bound Rab27a and coronin 3. We therefore consider that IQGAP1 plays a crucial role in the control of vesicle tethering and endocytosis by the recruitment of relevant regulators at each stage of the process (Fig. 5G).

Our data suggest that the conversion of Cdc42 in response to glucose regulates the dissociation of the tethering machinery and the subsequent formation of endocytic machinery. Glucose also regulates the dissociation of vesicle-tethering granuphilin/Slp4 from Rab27a and the subsequent formation of the coronin 3/GDP-bound Rab27a complex (1, 2). Thus, we consider that glucose stimulation promotes both fusion and dissociation events between the plasma membrane and the secretory membrane. In this study, we showed that glucose-induced formation of the complex, which comprises IQGAP1, GDP-bound Rab27a, and coronin 3, is necessary for endocytosis of the secretory membrane. Further studies are needed to investigate the dissociation mechanisms of this complex in pancreatic beta cells.

Biphasic endocytosis. IQGAP1 is also a GTP-dependent effector of Rac1, which belongs to the same family as Cdc42 (15, 16). In general, both GTP-bound Rac1 and Cdc42 interact with IQGAP1, and they are believed to play similar roles. We therefore confirmed the effect of Rac1 on the interaction between IQGAP1 and GDP-bound Rab27a. Rab27a-T23N bound IQGAP1 when the latter formed a complex with Rac1-G12V (Fig. 4A). Moreover, phogrin-

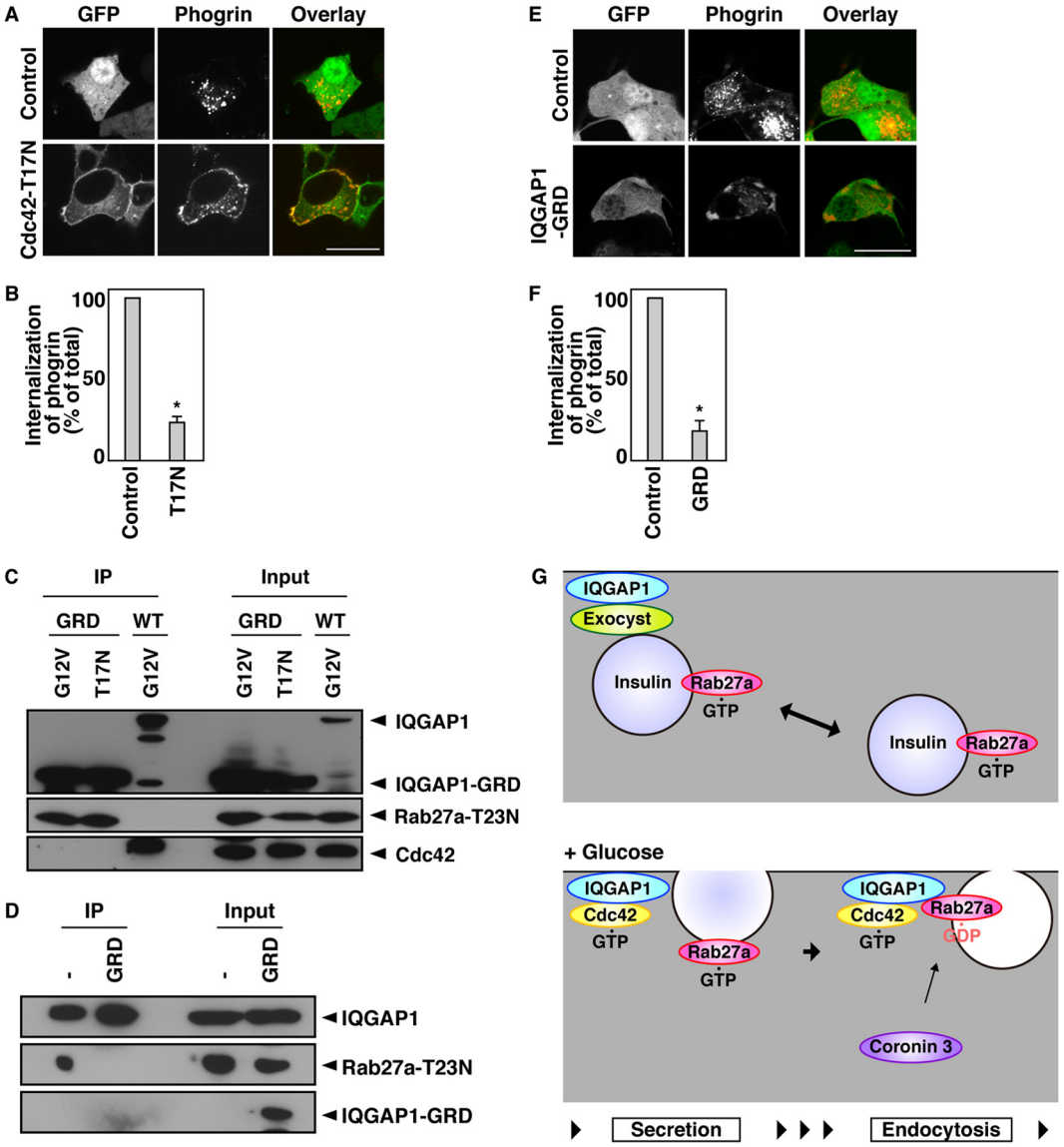

FIG 5 The complex consisting of IQGAP1 and GDP-bound Rab27a regulates endocytosis. (A) MIN6 cells expressing phogrin-Cherry together with GFP or GFP-Cdc42-T17N were incubated with 20 mM glucose for 5 min. (B) The percentage of transfected cells that had internalized phogrin-Cherry was analyzed by determination of the percentage of transfected cells that displayed cytoplasmic distribution of phogrin-Cherry fluorescence. (C) COS-7 extracts expressing Flag-Rab27a-T23N, either the G12V-Cdc42 or the T17N-Cdc42 mutant, and GFP-IQGAP1-WT or GFP-IQGAP1-GRD were immunoprecipitated with an anti-GFP antibody. The immunocomplexes were analyzed by immunoblotting using anti-GFP, anti-Flag, and anti-T7 antibodies. The percentage of input protein coimmunoprecipitated was 2.0%. (D) COS-7 extracts expressing Flag-IQGAP1, GFP-IQGAP1-GRD, and GFP-Rab27a-T23N were immunoprecipitated with an anti-Flag antibody. The immunocomplexes were analyzed by immunoblotting using anti-Flag and anti-GFP antibodies. The percentage of input protein coimmunoprecipitated was 0.2%. −, GFP. (E) MIN6 cells expressing phogrin-Cherry and either GFP or GFP-IQGAP1-GRD were incubated with 20 mM glucose for 5 min and were analyzed by immunofluorescence. Bars, 10 μm. (F) The percentage of transfected cells that had internalized phogrin-Cherry was analyzed by determination of the percentage of transfected cells that displayed cytoplasmic distribution of phogrin-Cherry fluorescence. The data in panels B and F were statistically analyzed as described in the legend to Fig. 3C. (G) Schematic model of IQGAP1 function in membrane trafficking.

Cherry was present near the plasma membrane in Rac1-T17N-expressing cells (data not shown). These results showed that Rac1 also promotes the complex formation that is necessary for endocytosis of the secretory membrane. In pancreatic beta cells, Rac1 may function at later steps in endocytosis, because the conversion of Rac1 in response to glucose is mediated by GTP-bound Cdc42 (12, 14). This finding raises the possibility that Cdc42 regulates rapid endocytosis while Rac1 regulates subsequent, prolonged endocytosis, a pattern that may be associated with the biphasic release of insulin in response to glucose. The rapid exocytosis is referred to as the first phase of insulin release, and the subsequent, less robust but sustained release is referred to as the second phase (46). This biphasic release of insulin suggests the presence of biphasic endocytosis, which is regulated by Cdc42 and Rac1 to maintain a constant cell volume. Further studies are required to investigate Cdc42- and Rac1-dependent endocytosis.

GDP-dependent effectors. IQGAP1 recruits GDP-bound Rab27a, as does GDI. Although IQGAP1 resembles GDI in terms

of this function, these two proteins appear to have different intracellular distributions. IQGAP1 is distributed in the vicinity of the plasma membrane and recruits GDP-bound Rab27a from the cytosol to the plasma membrane. GDI recruits GDP-bound GTPase from the plasma membrane to the cytosol and maintains the GTPase in the GDP-bound form (5–7). Moreover, IQGAP1 lacks the GDI consensus sequence. We therefore consider that IQGAP1 is a separate GDP-dependent effector. Interestingly, the binding properties of GDP-dependent effectors differ from those of classical GTP-dependent effectors; GDP-Rab27a simultaneously binds coronin 3 and IQGAP1, resulting in the formation of a trimeric complex.

Rab27a possesses both GTP- and GDP-dependent effectors. In pancreatic beta cells, GTP- and GDP-bound effectors regulate preexocytic and endocytic processes, respectively. This fact suggests that Rab27a regulates distinct stages in the insulin secretory pathway by changing its GDP/GTP-bound form and its binding partners. Since the physiological importance of GDP-binding proteins has been largely overlooked, we consider that other GTPases may also have GDP-dependent effectors.

ACKNOWLEDGMENTS

This research was supported by KAKENHI grants (19790636, 21790876, and 23791039), the Takeda Science Foundation, Novo Nordisk Pharma, and the Oita Broadcasting System Cultural Foundation and Research Fund at the Discretion of the President, Oita University.

We thank S. Seino (Kobe University), E. Kawasaki (Nagasaki University), and T. Senda and A. Shimomura (Fujita Health University) for providing plasmid constructs and J. Miyazaki (Osaka University) for providing the MIN6 cells. We also thank L. Kang, R. Nagata, A. Nakano, and Y. Oyama (Oita University) for helpful discussions and for the preparation of some materials and A. Satoh for technical assistance.

REFERENCES

1. **Kimura T, Niki I.** 2011. Rab27a in pancreatic beta-cells, a busy protein in membrane trafficking. Prog. Biophys. Mol. Biol. **107:**219–223.
2. **Kimura T, Niki I.** 2011. Rab27a, actin and beta-cell endocytosis. Endocr. J. **58:**1–6.
3. **Takai Y, Sasaki T, Matozaki T.** 2001. Small GTP-binding proteins. Physiol. Rev. **81:**153–208.
4. **Wennerberg K, Rossman KL, Der CJ.** 2005. The Ras superfamily at a glance. J. Cell Sci. **118:**843–846.
5. **Dirac-Svejstrup AB, Soldati T, Shapiro AD, Pfeffer SR.** 1994. Rab-GDI presents functional Rab9 to the intracellular transport machinery and contributes selectivity to Rab9 membrane recruitment. J. Biol. Chem. **269:** 15427–15430.
6. **Garrett MD, Zahner JE, Cheney CM, Novick PJ.** 1994. *GDI1* encodes a GDP dissociation inhibitor that plays an essential role in the yeast secretory pathway. EMBO J. **13:**1718–1728.
7. **Ullrich O, Horiuchi H, Bucci C, Zerial M.** 1994. Membrane association of Rab5 mediated by GDP-dissociation inhibitor and accompanied by GDP/GTP exchange. Nature **368:**157–160.
8. **Novick P, Zerial M.** 1997. The diversity of Rab proteins in vesicle transport. Curr. Opin. Cell Biol. **9:**496–504.
9. **Fukui K, Sasaki T, Imazumi K, Matsuura Y, Nakanishi H, Takai Y.** 1997. Isolation and characterization of a GTPase activating protein specific for the Rab3 subfamily of small G proteins. J. Biol. Chem. **272:**4655–4658.
10. **Kowluru A.** 2010. Small G proteins in islet beta-cell function. Endocr. Rev. **31:**52–78.
11. **Kowluru A, Seavey SE, Li G, Sorenson RL, Weinhaus AJ, Nesher R, Rabaglia ME, Vadakekalam J, Metz SA.** 1996. Glucose- and GTP-dependent stimulation of the carboxyl methylation of CDC42 in rodent and human pancreatic islets and pure beta cells. Evidence for an essential role of GTP-binding proteins in nutrient-induced insulin secretion. J. Clin. Invest. **98:**540–555.
12. **Nevins AK, Thurmond DC.** 2003. Glucose regulates the cortical actin network through modulation of Cdc42 cycling to stimulate insulin secretion. Am. J. Physiol. Cell Physiol. **285:**C698–C710.
13. **Nevins AK, Thurmond DC.** 2005. A direct interaction between Cdc42 and vesicle-associated membrane protein 2 regulates SNARE-dependent insulin exocytosis. J. Biol. Chem. **280:**1944–1952.
14. **Wang Z, Oh E, Thurmond DC.** 2007. Glucose-stimulated Cdc42 signaling is essential for the second phase of insulin secretion. J. Biol. Chem. **282:**9536–9546.
15. **Hart MJ, Callow MG, Souza B, Polakis P.** 1996. IQGAP1, a calmodulin-binding protein with a rasGAP-related domain, is a potential effector for cdc42Hs. EMBO J. **15:**2997–3005.
16. **Kuroda S, Fukata M, Kobayashi K, Nakafuku M, Nomura N, Iwamatsu A, Kaibuchi K.** 1996. Identification of IQGAP as a putative target for the small GTPases, Cdc42 and Rac1. J. Biol. Chem. **271:**23363–23367.
17. **Briggs MW, Sacks DB.** 2003. IQGAP proteins are integral components of cytoskeletal regulation. EMBO Rep. **4:**571–574.
18. **Fukata M, Nakagawa M, Itoh N, Kawajiri A, Yamaga M, Kuroda S, Kaibuchi K.** 2001. Involvement of IQGAP1, an effector of Rac1 and Cdc42 GTPases, in cell-cell dissociation during cell scattering. Mol. Cell. Biol. **21:**2165–2183.
19. **Fukata M, Nakagawa M, Kaibuchi K.** 2003. Roles of Rho-family GTPases in cell polarisation and directional migration. Curr. Opin. Cell Biol. **15:**590–597.
20. **Fukata M, Watanabe T, Noritake J, Nakagawa M, Yamaga M, Kuroda S, Matsuura Y, Iwamatsu A, Perez F, Kaibuchi K.** 2002. Rac1 and Cdc42 capture microtubules through IQGAP1 and CLIP-170. Cell **109:**873–885.
21. **Noritake J, Fukata M, Sato K, Nakagawa M, Watanabe T, Izumi N, Wang S, Fukata Y, Kaibuchi K.** 2004. Positive role of IQGAP1, an effector of Rac1, in actin-meshwork formation at sites of cell-cell contact. Mol. Biol. Cell **15:**1065–1076.
22. **Rittmeyer EN, Daniel S, Hsu SC, Osman MA.** 2008. A dual role for IQGAP1 in regulating exocytosis. J. Cell Sci. **121:**391–403.
23. **Nauert JB, Rigas JD, Lester LB.** 2003. Identification of an IQGAP1/AKAP79 complex in β-cells. J. Cell. Biochem. **90:**97–108.
24. **Fukuda M.** 2005. Versatile role of Rab27 in membrane trafficking: focus on the Rab27 effector families. J. Biochem. **137:**9–16.
25. **Grosshans BL, Ortiz D, Novick P.** 2006. Rabs and their effectors: achieving specificity in membrane traffic. Proc. Natl. Acad. Sci. U. S. A. **103:** 11821–11827.
26. **Zerial M, McBride H.** 2001. Rab proteins as membrane organizers. Nat. Rev. Mol. Cell Biol. **2:**107–117.
27. **Izumi T, Gomi H, Kasai K, Mizutani S, Torii S.** 2003. The roles of Rab27 and its effectors in the regulated secretory pathways. Cell Struct. Funct. **28:**465–474.
28. **Mizuno K, Ramalho JS, Izumi T.** 2011. Exophilin8 transiently clusters insulin granules at the actin-rich cell cortex prior to exocytosis. Mol. Biol. Cell **22:**1716–1726.
29. **Waselle L, Coppola T, Fukuda M, Iezzi M, El-Amraoui A, Petit C, Regazzi R.** 2003. Involvement of the Rab27 binding protein Slac2c/MyRIP in insulin exocytosis. Mol. Biol. Cell **14:**4103–4113.
30. **Kotake K, Ozaki N, Mizuta M, Sekiya S, Inagaki N, Seino S.** 1997. Noc2, a putative zinc finger protein involved in exocytosis in endocrine cells. J. Biol. Chem. **272:**29407–29410.
31. **Matsumoto M, Miki T, Shibasaki T, Kawaguchi M, Shinozaki H, Nio J, Saraya A, Koseki H, Miyazaki M, Iwanaga T, Seino S.** 2004. Noc2 is essential in normal regulation of exocytosis in endocrine and exocrine cells. Proc. Natl. Acad. Sci. U. S. A. **101:**8313–8318.
32. **Gomi H, Mizutani S, Kasai K, Itohara S, Izumi T.** 2005. Granuphilin molecularly docks insulin granules to the fusion machinery. J. Cell Biol. **171:**99–109.
33. **Torii S, Zhao S, Yi Z, Takeuchi T, Izumi T.** 2002. Granuphilin modulates the exocytosis of secretory granules through interaction with syntaxin 1a. Mol. Cell. Biol. **22:**5518–5526.
34. **Wang J, Takeuchi T, Yokota H, Izumi T.** 1999. Novel rabphilin-3-like protein associates with insulin-containing granules in pancreatic beta cells. J. Biol. Chem. **274:**28542–28548.
35. **Kimura T, Kaneko Y, Yamada S, Ishihara H, Senda T, Iwamatsu A, Niki I.** 2008. The GDP-dependent Rab27a effector coronin 3 controls endocytosis of secretory membrane in insulin-secreting cell lines. J. Cell Sci. **121:** 3092–3098.
36. **Kimura T, Taniguchi S, Toya K, Niki I.** 2010. Glucose-induced translocation of coronin 3 regulates the retrograde transport of the secretory

membrane in the pancreatic β-cells. Biochem. Biophys. Res. Commun. **395:**318–323.
37. **Kimura T, Taniguchi S, Niki I.** 2010. Actin assembly controlled by GDP-Rab27a is essential for endocytosis of the insulin secretory membrane. Arch. Biochem. Biophys. **496:**33–37.
38. **Fukata M, Kuroda S, Fujii K, Nakamura T, Shoji I, Matsuura Y, Okawa K, Iwamatsu A, Kikuchi A, Kaibuchi K.** 1997. Regulation of cross-linking of actin filament by IQGAP1, a target for Cdc42. J. Biol. Chem. **272:** 29579–29583.
39. **Kuroda TS, Fukuda M.** 2004. Rab27A-binding protein Slp2-a is required for peripheral melanosome distribution and elongated cell shape in melanocytes. Nat. Cell Biol. **6:**1195–1203.
40. **Kuroda TS, Fukuda M, Ariga H, Mikoshiba K.** 2002. The Slp homology domain of synaptotagmin-like proteins 1–4 and Slac2 functions as a novel Rab27A binding domain. J. Biol. Chem. **277:**9212–9218.
41. **Torii S, Saito N, Kawano A, Zhao S, Izumi T, Takeuchi T.** 2005. Cytoplasmic transport signal is involved in phogrin targeting and localization to secretory granules. Traffic **6:**1213–1224.
42. **Vo YP, Hutton JC, Angleson JK.** 2004. Recycling of the dense-core vesicle membrane protein phogrin in Min6 β-cells. Biochem. Biophys. Res. Commun. **324:**1004–1010.
43. **Watanabe T, Wang S, Noritake J, Sato K, Fukata M, Takefuji M, Nakagawa M, Izumi N, Akiyama T, Kaibuchi K.** 2004. Interaction with IQGAP1 links APC to Rac1, Cdc42, and actin filaments during cell polarization and migration. Dev. Cell **7:**871–883.
44. **Brandt DT, Marion S, Griffiths G, Watanabe T, Kaibuchi K, Grosse R.** 2007. Dia1 and IQGAP1 interact in cell migration and phagocytic cup formation. J. Cell Biol. **178:**193–200.
45. **Kasai K, Fujita T, Gomi H, Izumi T.** 2008. Docking is not a prerequisite but a temporal constraint for fusion of secretory granules. Traffic **9:**1191–1203.
46. **Curry DL, Bennett LL, Grodsky GM.** 1968. Dynamics of insulin secretion by the perfused rat pancreas. Endocrinology **83:**572–584.